Earthquake Geotechnical Engineering for Protection and Development of Environment and Constructions – Silvestri & Moraci (Eds)
© 2019 Associazione Geotecnica Italiana, Rome, Italy, ISBN 978-0-367-14328-2

Assessment of the microstructure effects on the site dynamic response of residual soils

N.C. Pete Vargas
Engineering Department, DICEIN S.A.S Consulting Engineers, Bogotá D.C., Colombia.
Universidad Nacional de Colombia, Bogotá D.C., Colombia

J.A. Pineda Jaimes
Research Centre for Sustainable Engineering CIDIS Bogota D.C., Colombia.
Department of Civil and Agricultural Engineering, Universidad Nacional de Colombia, Bogotá D.C., Colombia

J.E. Colmenares
Department of Civil and Agricultural Engineering, Universidad Nacional de Colombia Bogotá D.C., Colombia

It has been widely recognized that parameters usually used to characterize de dynamic behavior of geomaterials (G/G_{max}, D/D_{min}, γ, V_s), in small strain domain ($\gamma<10^{-3}$), are controlled primarily by the confinement level, the type of material and the microstructure (arrangement of particles + interparticle forces). In residual soils, the development of chemical weathering controls microstructural features and plays a fundamental role in the dynamic response of weathering profiles. The effect of microstructure in seismic ground movements of residual soils was studied by using a linear equivalent site dynamic response for two strong earthquakes. Two soil profiles were analyzed in which the dynamic properties of the soil profiles were established via resonant column testing for natural microstructured and destructured states, incorporating the effects of capillary (matric suction) forces. It was found that the effects of matric suction and net confinement is low in ground motion parameters, compared with those of cementation and particle bonding. Dynamic analysis is emerging as a novel tool for the study of the effects of microstructure in geotechnical problems.

1 INTRODUCTION

The north western region of Colombia (South America) is a tectonically active area. It has recently experienced strong seismic events that have caused considerable damage in many cities and populated areas. In that area of the country, it is common to find deep weathering profiles of residual soils formed from in-situ weathering of intrusive igneous rocks and crystalline metamorphic rocks. Those rocks have been the object of several studies due to their particular behaviour according to the intensity of weathering (Pineda, 2011; Pineda, Colmenares, & Hoyos, 2014). The dynamic response in free field for a typical weathering profile of this area was evaluated. The effect of microstructure (fabric, interparticle bonding and capillary forces) on the strong ground motion parameters was studied for a typical weathered profile.

A comparative analysis considering suction and net confinement was made. It studied the site response of a typical natural weathering profile derived from a granodiorite and the site response of an equivalent synthetic profile in which the properties of stiffness and damping were established experimentally for the same materials in destructured conditions. The strong

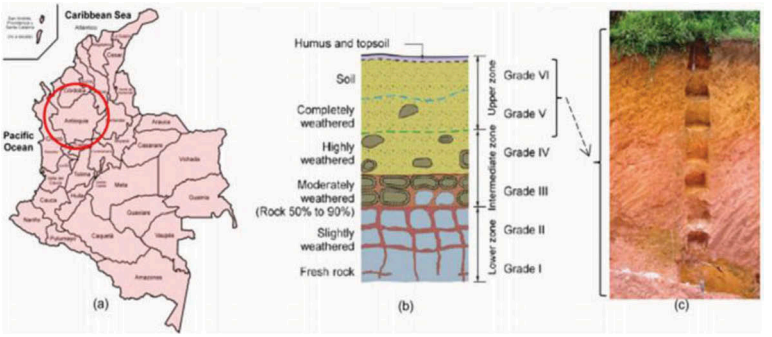

Figure 1. Exploration zone: (a) geographic location, (b) igneous rock weathering profile and (c) weathering profile in the study area.
Adapted from (Pineda et al., 2014).

Table 1. Materials for different degrees of weathering.

Horizon in the Weathering profile	Degree of weathering of the specific horizon	Material for a given degree of weathering
Upper Horizon	Grade VI	Residual soil
	Grade V	Fully weathered rock
Intermediate Horizon	Grade IV	Highly weathered rock
	Grade III	Moderately weathered rock (proportion of intact rock blocks in relation to total volume 50% - 90%)
Lower Horizon	Grade II	Weathered rock
	Grade I	Unweathered rock

* *Own preparation, modified from* (Pineda, 2011)

ground motion parameters that were used for the analysis are the response spectra in terms of Spectral Accelerations (*Sa*), Peak Ground Accelerations (*PGA*), the energy released from the Arias Intensity (*AI*) concept and the Amplification Factor (F_{PGA}) with respect to the signal input at the base of the soil profiles, where the intact rock is located. The dynamic analysis carried out is presented as a tool for understanding the effect of the microstructure in small-strain dynamic response of soils. The typical weathering profile of igneous rocks is presented in Table 1 (Anon, 1995) and in Figure 1 (b). In the soil profiles analysed, the two shallower horizons were studied with more emphasis. They correspond to materials with weathering grades of VI (residual soil) and V (saprolites).

2 DEFINITION OF PARAMETERS FOR DYNAMIC RESPONSE ANALYSIS

Dynamic response analysis was carried out for two soil profiles with the following characteristics:

Natural Profile (NP): A weathering soil profile with residual soils characterized by a microstructure as found by in-situ conditions derived from the weathering process (fabric, matric suction and intergranular cementation or bonding with sesquioxides (Pineda et al., 2014). Dynamic properties at small-strain range were established via Resonant Column (RC) testing in the linear range, at constant water content (Pineda et al., 2014; Pineda, Hoyos, & Colmenares, 2010).

Synthetic Profile (SP): Corresponds to properties of the soils conforming the Natural Profile, but without the influence of the soil microstructure and bonded links between particles. Samples of statically compacted materials were prepared from the soils of the weathering profile. They used destructured materials at similar natural void ratio (e_o) in order to control

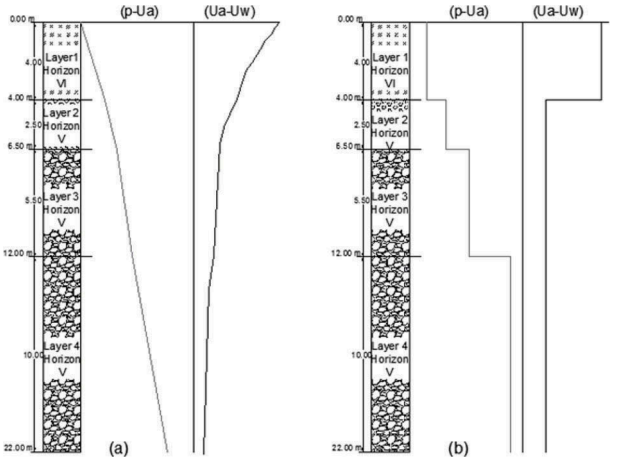

Figure 2. Diagram of profiles analyzed: (a) natural profile (*NP*), (b) synthetic profile (*SP*).

some variables such as matric suction, and net confining stress (Hoyos, Suescún, Pineda, & Puppala, 2010; Pineda & Pete, 2017; Pino, 2013).

Figure 2, shows schematically the variation with depth of capillary forces (matric suction) and net confinement level (p-U_a) for both soil profiles. At the bottom of layer 4, the intact rock and seismic input signals were located.

2.1 *Definition of the natural soil profile (NP)*

The properties of residual soils from the natural profile *(NP)* can be found in table 2. They were established from different studies carried out on this type of soils (Barrera, 2010; Pineda, 2011; Pineda et al., 2010; Pineda et al, 2014). The soil profile was evaluated down to a depth of 22.00m.

Table 2 shows the index properties of soils in their natural state: total unit weight (γ_t), gravimetric water content (ω_n), average net normal stress (p-U_a), specific gravity (G_s), void ratio (e_o), degree of saturation (S) and volumetric water content (Θ).

Table 2. Natural profile (NP) properties for residual soil.

Layer	Horizon	Depth (m)			Average depth (m)	γ_t (KN/m^3)	ω_n (%)	(p-U_a) (KN/m^2)	G_S	e_o	S (%)	Θ (%)	Vs (m/s)
1	VI	0.00	-	2.00	1.00	18.47	18.2	12.79	2.61	0.67	73%	29.5%	75
	VI	2.00	-	3.00	2.50	18.12	21.35	31.36	2.61	0.79	75%	33.1%	
	VI	3.00	-	4.00	3.50	18.12	22.17	43.91	2.62	0.81	80%	35.6%	
2	V	4.00	-	6.50	5.00	16.44	23.56	56.91	2.68	0.9	73%	34.4%	98
3	V	6.50	-	8.00	7.00	17.68	24.15	85.68	2.70	0.91	71%	33.7%	100
	V	8.00	-	10.00	9.00	17.80	25.00	110.91	2.70	0.95	73%	35.6%	
	V	10.00	-	12.00	11.00	18.50	21.50	140.89	2.70	0.95	66%	31.9%	
4	V	12.00	-	14.00	13.00	19.50	24.50	175.50	2.71	0.96	70%	34.1%	150
	V	14.00	-	16.00	15.00	19.85	17.00	206.14	2.80	0.96	60%	29.3%	
	V	16.00	-	18.00	17.00	19.85	18.45	233.62	2.80	0.96	62%	30.3%	
	V	18.00	-	20.00	19.00	20.00	18.90	263.07	2.80	0.98	62%	30.7%	
	V	20.00	-	22.00	21.00	20.00	22.50	290.77	2.80	0.98	67%	33.2%	

* *Own elaboration, properties taken of* (Barrera, 2010; Pineda, 2011; Pineda et al., 2010)

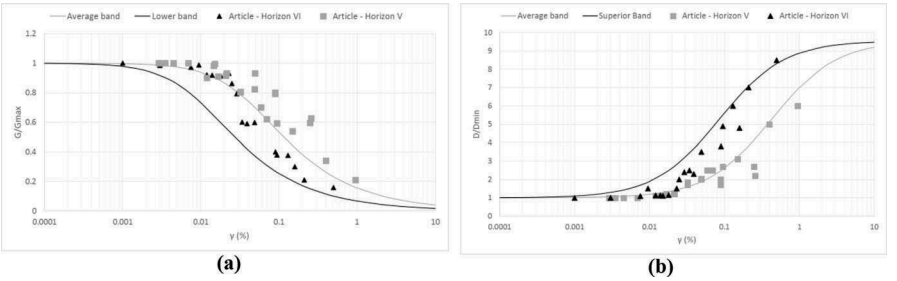

Figure 3. Experimental data of shear modulus degradation and damping ratio. Own elaboration based on the results of (adapted from Pineda, 2011; Pineda et al., 2014).

Resonant Column testing, at constant water content, allowed to establish the dynamic response in terms of (G/G_{max}) y (D/D_{min}) for each horizon (see Figure 3).

Equations (1) and (2) were used for adjustment of the dynamic stiffness and damping degradation curves. The fitting parameters are presented in table 3. Materials of the horizon (VI) can be described as silt of low plasticity (ML) with the presence of iron and aluminium oxides acting as cementing bonds in the fabric. Soils of horizon (V), are composed by silty sands (SM) with links between particles of kaolinite and other secondary minerals derived from the partial weathering of feldspars and amphiboles, which do not represent rigid cemented bonds (Pineda, 2011; Pineda et al., 2014). Figure 4 shows the water retention curves of the materials in the natural state, established for a drying process. The filter paper method was used for the measurement of matric suction (Barrera, 2010).

$$\frac{G}{G_{max}} = \frac{1}{\left[1 + \left(\frac{\gamma}{\gamma_Y}\right)^n\right]^m} \tag{1}$$

Table 3. Parameters for definition of damping and modulus degradation curves.

	Degradation curve modulus (G/G_{max})				Damping (D)			
Formation	N	m	$\gamma_{r(max)}$	$\gamma_{r(min)}$	D_{min}	D_{max}	$\gamma_{r(max)}$	$\gamma_{r(min)}$
S.R Granodiorite and Cuarzodiorite	1.30	0.45	0.075	0.010	4.01	28.38	0.01	0.090

* *Own elaboration, properties taken of* (Jaramillo, Villarraga, Farbiarz, Vélez, & Restrepo, 2006)

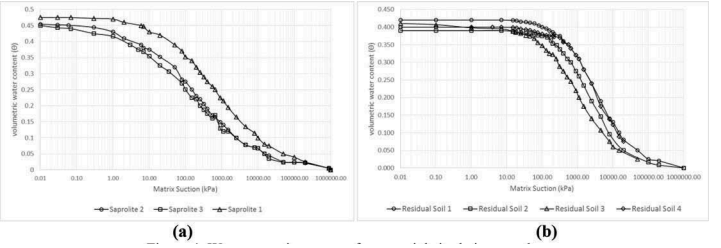

Figure 4. Water retention curves for materials in their natural state. (a) Horizon V, (b) Horizon VI. Own elaboration based on Barrera (2010).

Table 4. Properties for the synthetic profile (SP) established for the modelling

Layer	Horizon	Depth (m)	Average depth (m)	γ_t (kN/m^3)	$(p\text{-}U_a)$ (kN/m^2)	$(p\text{-}U_a)$ Adopted (kPa)	Θ (%)	$(U_a\text{-}U_w)$ (kPa)	$(U_a\text{-}U_w)$ adopted (kPa)	Vs (m/s)
1	VI	0.00 - 2.00	1.00	12.24	25.6	25	29.5%	275	200	141
	VI	2.00 - 3.00	2.50				33.1%			
	VI	3.00 - 4.00	3.50				35.6%			
2	V	4.00 - 6.50	5.25	16.92	57.0	50	34.4%	36	50	378
3	V	6.50 - 8.00	7.25	18.02	111.0	100	33.7%			
		8.00 - 10.00	9.00				35.6%			
		10.00 - 12.00	11.00				31.9%			
4	V	12.00 - 14.00	13.00	19.84	233.6	200	34.1%			
		14.00 - 16.00	15.00				29.3%			
		16.00 - 18.00	17.00				30.3%			
		18.00 - 20.00	19.00				30.7%			
		20.00 - 22.00	21.00				33.2%			

* *Own elaboration, properties taken from* (Barrera, 2010; Hoyos et al 2010; Pineda, 2011; Pino, 2013)

$$D = D_{min} + \frac{\frac{\gamma}{\gamma_{min}}}{\frac{1}{D_{min}}\frac{\frac{\gamma}{\gamma_{min}}}{D_{max}+D_{min}}} \tag{2}$$

2.2 *Definition of the synthetic profile (SP)*

Based on the volumetric water content established for the weathered materials, the water retention curves established by Barrera (2010) were used to establish the matric suction in each horizon. In order to reproduce a synthetic profile (*SP*), of destructured materials, the values of $(p\text{-}U_a)$ and $(U_a\text{-}U_w)$ established experimentally in the tests of resonant column with suction control were included (Hoyos et al 2010, Pino 2013). Table 4 shows the main parameters established for (*SP*) profile.

Constant matric suction and net confinement $(p\text{-}U_a)$ values were established for each weathering horizon. In order to obtain the curves G/G_{max} and D/D_{min}, affected by suction and net confinement, but without bonding in the fabric, the studies carried out by (Pino, 2013) and (Hoyos et al, 2010) were used. They studied the soil behaviour at constant suction in RC equipment. Soils from the natural profile were compacted at void ratios similar to the natural

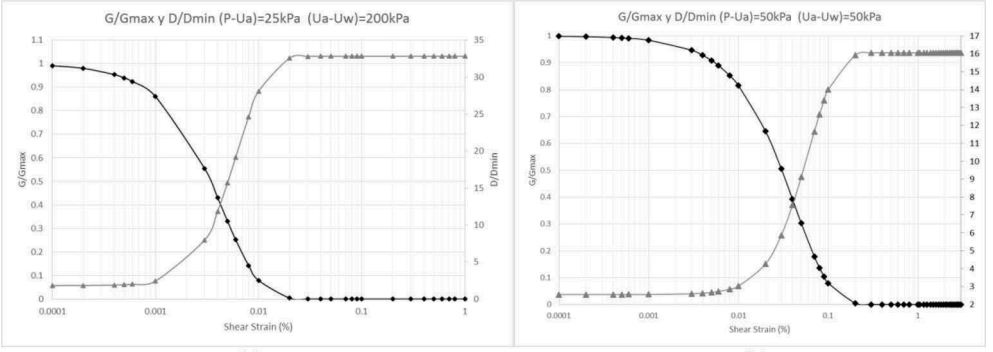

(a) **(b)**

Figure 5. Modulus degradation curves and damping ratio: (a) Horizon VI, layer I, (b) Horizon V layer 2. Own elaboration, based on data from (Pino, 2013 and Hoyos et al, 2010).

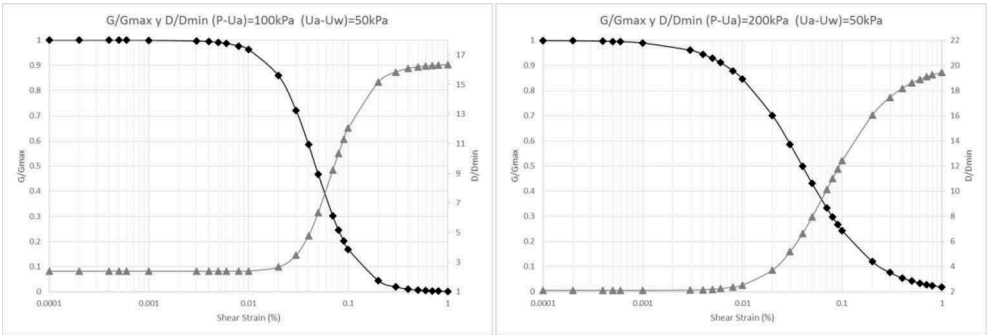

(a) **(b)**

Figure 6. Modulus degradation curves and damping ratio: (a) Horizon V, layer 3, (b) Horizon V layer 4. Own elaboration, based on the results of (Pino, 2013 and Hoyos et al, 2010).

values. Figures 5 and 6 show the curves of the dynamic response (adapted from (Pineda & Pete, 2017), including some additional points obtained by Pineda et al. (2010).

2.3 *Definition of seismic signals*

According to the accelerations levels established in the studied region (0.15g to 0.20g from seismic hazard studies), signals of real earthquakes were taken with maximum accelerations within this range for the simulation of site response. First signal corresponds to the North-ridge earthquake and the second one corresponds to theChiChi earthquake. They were

Table 5. Characteristics of the seismic signals used

Earthquake	Year	Epicenter	Location	PGA (g)	PGV (m/s)	PGD (m)	t(s)	Magnitude
Northridge	1994	Reseda, LA	Northdridge, EEUU	0.22	0.098	0.028	7.1	6.7
ChiChi	1999	ChiChi, Nantou	Nantau. Taiwan	0.18	0.39	0.1	17.88	7.3

* *Own elaboration, Signals taken from (PEER)*

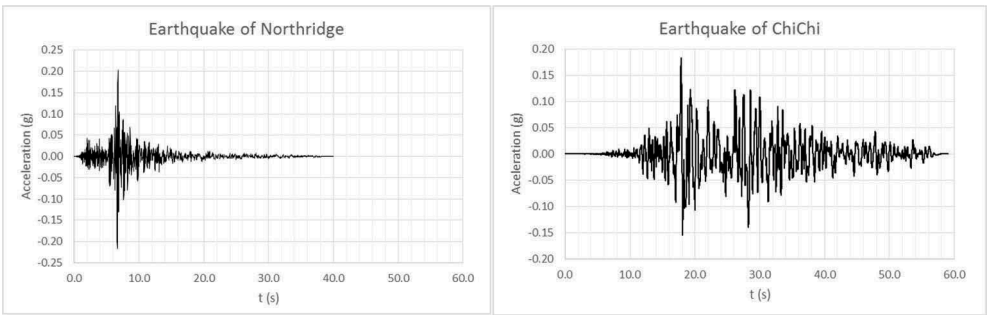

(a) **(b)**

Figure 7. Seismic signals used for the dynamic modelling of the soil profile (Hashash et al., 2018).

selected from the Pacific Earthquake Engineering Research Center (PEER) database. Table 5 shows the main characteristics of each of these seismic events and in figure 7, time acceleration histories are presented. Northridge signal presents a shorter duration than the ChiChi event, despite the similarities in maximum values of acceleration recorded.

One dimensional modelling was performed using an equivalent linear model in the frequency domain. The signal was applied the lower boundary of the layer 4, assuming rock rigid behaviour and total reflection of seismic waves.

3 ANALYSIS OF RESULTS AND DISCUSSION

3.1 *Response Spectrum in terms of (S_a)*

Figure 8, shows the response spectra in terms of (S_a) for each defined layer for (*NP*) and (*SP*) profiles. It is evident that (S_a) for both seismic signals in the synthetic profile (*SP*) exhibit lower peak values than those of the natural profile (*NP*). This tendency is clearly seen in layer 1 (horizon VI) (see Fig 8a). It is probably due to the fact that in the (*NP*) profile the microstructure, of soils derived from weathering, has a smaller energy dissipation capacity.

It can be observed that peak (S_a) values for (*SP*) profile, in all layers (horizons VI and V through profiles, figs 8a to 8d) are very similar irrespective of the net confinement level and the matric suction imposed. Apparently these variables have no effect in the dynamic response of the soil in destructured states. Variations in matric suction do not produce great changes in (S_a). It can be seen by comparing figure 8a with 8b, where suction changes from 200kPa to 50kPa respectively. The difference in the peak values of (S_a) for each profile can be attributed to cemented bonds and the effect of the microstructure generated in horizons VI (layer 1), where bonding is more stronger than horizon (V) (Pineda et al., 2014). This is confirmed by the observation that increasing net normal confinement in horizon (V) originates similarly response spectra in (*NP*) and (*SP*) profiles.

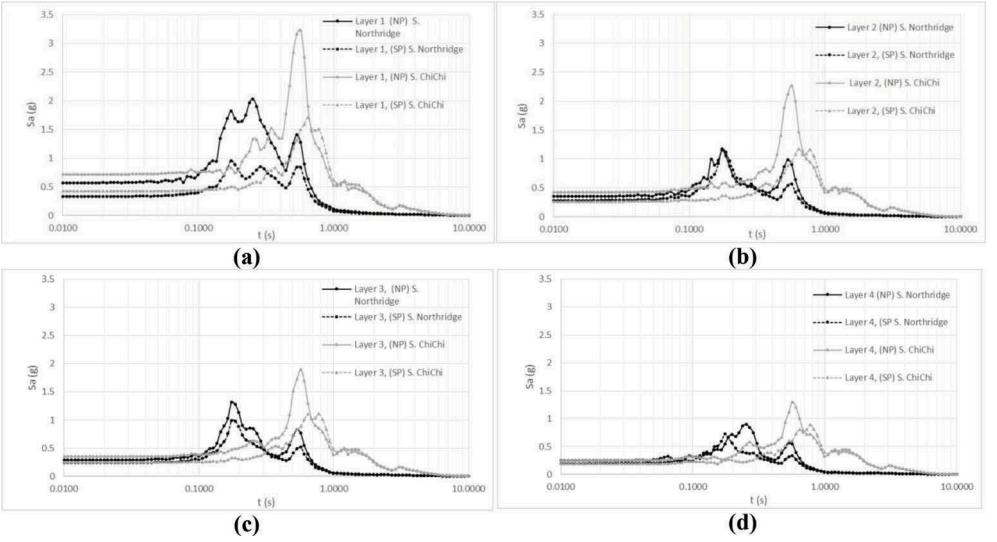

Figure 8. Spectra of response to Northdridge and ChiChi seismic signals for (PN) and (PS) respectively: (a) Layer 1, (b) Layer 2, (c) layer 3 and (d) layer 4.

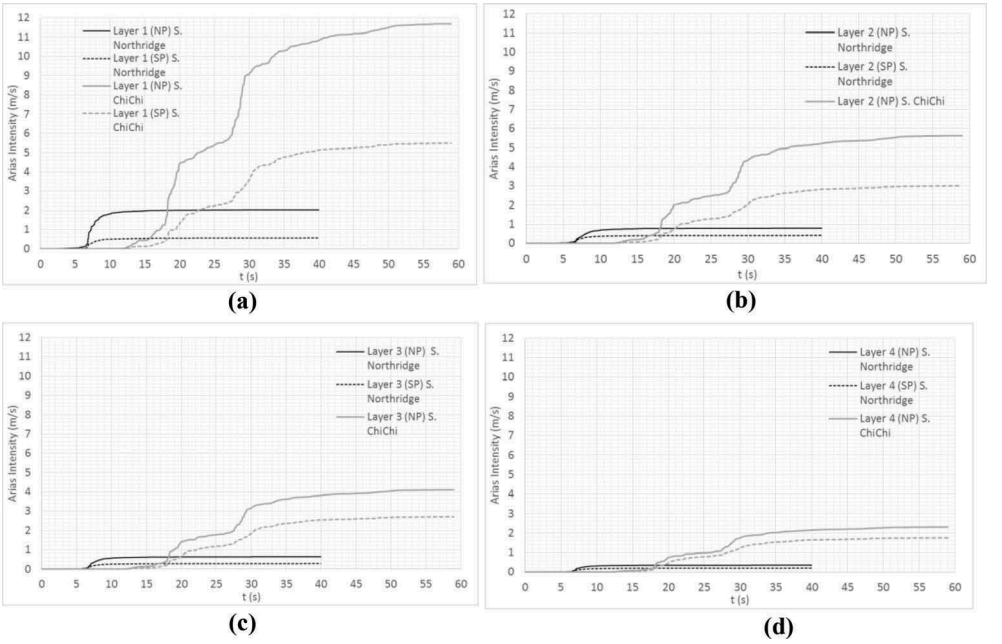

Figure 9. Arias Intensity values for Northridge and ChiChi seismic signals for each profile (*NP*) and (*SP*). (a) Layer 1, (b) Layer 2, (c) layer 3 and (d) layer 4.

3.2 *Arias Intensity (AI)*

Arias Intensity (AI), is defined as the energy accumulated in relation to the energy that is absorbed in the ground during a seismic movement (Travasarou, Bray, & Abrahamson, 2003). That is, the energy dissipated per unit of weight in the soil profile during a seismic event. This parameter has units of speed and is usually expressed in meters per second (m/s), as shown in Equation 3.

$$I_A = \frac{\pi}{2g}\int_0^{T_d} a(t)^2 dt \quad \left(\frac{m}{s}\right) \tag{3}$$

Figure 9 presents the comparative results of (AI), for each layer including both natural (*NP*) and synthetic (*SP*) profiles.

In Figures 9a - 9d, it can be observed that, in the natural profile (*NP*), the energy dissipation rate for layer 1 (horizon VI) is lower than for other layers (Horizon V). For the synthetic profile (*SP*), the dissipation values in all layers are similar and smaller than the natural ones. All over the soil profile, a similar tendency to that found in the spectra is observed. The upper layer has a more rigid microstructure with respect to other layers. The energy dissipation coefficient (AI) between the (*NP*) and (*SP*) values decreases with depth for all layers. Additionally, it is clear that for signals with a long period, such as the ChiChi earthquake, the capacity of energy dissipation becomes smaller, so the duration of the event in terms of (AI) is more important than peak acceleration of the signal.

3.3 *Analysis of F_{PGA} and PGA*

The amplification factor F_{PGA} is the ratio between the maximum acceleration value produced in any layer and the maximum acceleration value generated in the base $F_{PGA}=PGA_m/PGA_b$. This factor indicates whether the signal, in terms of accelerations, is amplified or attenuated in

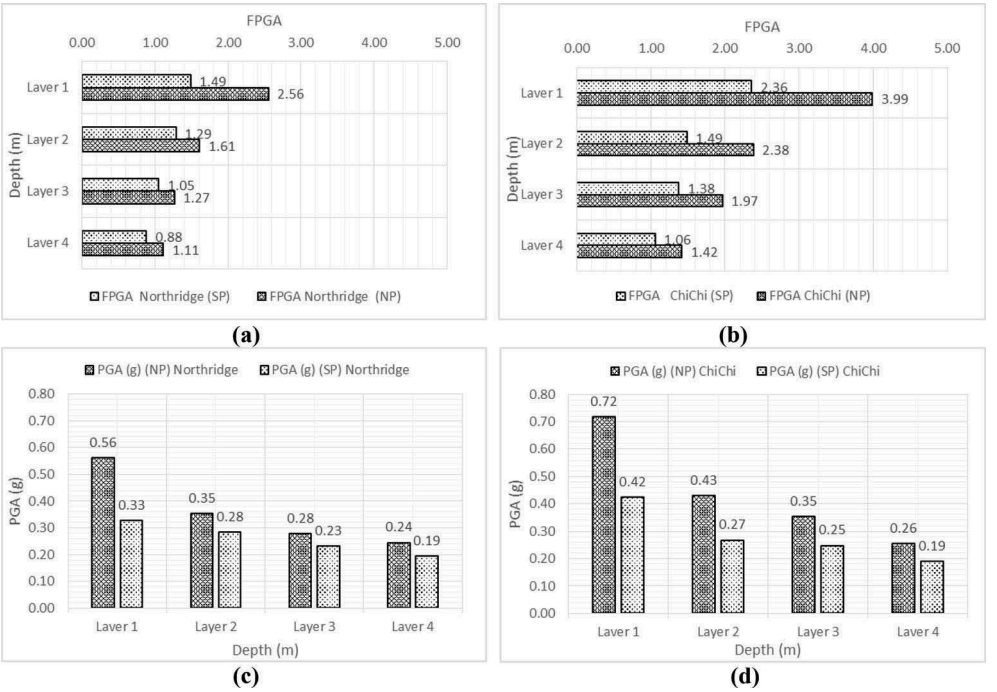

Figure 10. PGA results and the F_{PGA} amplification factor for each layer: (a) Northridge earthquake F_{PGA}, (b) ChiCHi earthquake F_{PGA}, (c) Northridge earthquake PGA, (d) PGA for ChiChi earthquake.

the soil profile, with respect to the acceleration of the signal in the rock (Pete & Pineda, 2018). The PGA was evaluated for both earthquakes in each layer. Figure 10, shows that when the confinement level increases, both in *(NP)* and *(SP)* profiles, the F_{PGA} factor and PGA peak acceleration decreases with respect to the values of layer 1. Similar trends were found by (Pete & Pineda, 2018), therefore, signals of ChiChi and Northridge earthquakes, in both profiles, are amplified. However, for ChiChi earthquake greater amplifications are observed in comparison with Northridge earthquake where the accelerations in the base are greater than in ChiChi earthquake. That is, the duration of the seismic event directly affects the surface response. Similarly, this behaviour can be related to the effects of suction, by comparing the graph (c) and (d) where the Chichi earthquake shows a more marked difference for the peak accelerations between layer 1 and 2 of the (SP) than in the Northridge earthquake. Assuming that this profile, in theory, presents the same fabric and it is not affected by bonding, the suction probably affects more representatively the dynamic response for long-term earthquakes.

4 SUMMARY AND CONCLUSIONS

Non-linear elastic simulations were performed in order to understand the influence of microstructure on seismic movements in free field conditions for two residual soils with different weathering intensities. The dynamic response analyses were carried out considering previous experimental results whose soils had different fabric conditions, matric suction and net confinement level. Those conditions were included in a natural soil profile (*NP*) and its synthetic equivalent profile (*SP*). In both soil profiles, it was observed that for the longest analysed earthquake (ChiChi), greater spectral accelerations were reached in the surface (layer 1) than for the shorter duration earthquake (Northridge). This suggests that the duration of the seismic event and the stiffness nature of the medium, controlled by microstructure, in which the

waves propagate, determine the magnitude of the seismic movements at the surface, even though the accelerations in rock are different. For both (NP) and (SP) profiles, the energy released from the earthquake decreases between layers 1 to 4. Also, the difference in the magnitude of the energy released at any time for (NP) and (SP) decreases with the increase in the level of confinement. This tendency is reflected in higher values of PGA and FPGA for all the layers analysed in the natural profile. The effects of microstructure (considering capillary forces and interparticle bonding) on the dynamic surface response (layer 1) are more relevant in the natural profile (NP), since maximum spectral accelerations (S_a) occurs in that condition. Destructuring of the materials, which mainly leads to the breaking of cement bonds and the modification of the fabric means that the energy dissipation capacity of the synthetic profile (*SP*) is greater; therefore, the confinement level and the imposed suction for those materials determine the dynamic response in all layers. Since there are no rigid bonds in the microstructure of the residual soil with the degree of weathering (V), the spectral response for layers 2, 3 and 4 are similar in both the natural profile (*NP*) and the synthetic profile (*SP*).

Dynamic analysis is emerging as a novel tool for the study of the effects of microstructure in seismic geotechnical problems. Given that the presence of microstructure modifies the energy dissipation capacity of soils, it is necessary to go deeper into the evaluation of the microstructure when performing site response analyses. It will incorporate more realistic ground response analysis in the determination of the seismic movements for structural design of structures in this type of materials.

REFERENCES

Anon. (1995). The description and classification of weathered rocks for engineering purposes. *Quarterly Journal of Engineering Geology*, *28*, 207–242.

Barrera, N. (2010). *Influence of weathering on the hydraulic conductivity function of residual soil derived from an igneous rock*. Universidad Nacional de Colombia.

Hashash, Y. M. A., Musgrove, M. I., Harmon, J. A., Okan, I., Groholski, D. R., Phillips, C. A., & Park, D. (2018). DEEPSOIL 7.0, User Manual, 1–169.

Hoyos, L., Suescún, E., Pineda, J., & Puppala, A. (2010). Small-strain stiffness of compacted silty sand using a proximitor-based suction-controlled resonant column device. In *Fifth International Conference* … (pp. 683–688). https://doi.org/10.13140/RG.2.1.4255.7284

Jaramillo, J. D., Villarraga, M., Farbiarz, Y., Vélez, A., & Restrepo, L. (2006). *Microzonificación sísmica detallada de los municipios de Barbosa, Girardota, Copacabana, Sabaneta, La Estrella, Caldas y Envigado*. Medellín, Antioquia - Colombia.

Pete, N., & Pineda, J. (2018). Influence of thinckness of an unsaturated soil deposit on dynamic response of a strong earthquake, (October).

Pineda, J. (2011). *Influence of Weathering on Stress- Strain Behaviour and Small-strain Stiffness of Residual Soils Derived from a Granodiorite (in Spanish*). Universidad Nacional de Colombia.

Pineda, J., Colmenares, J., & Hoyos, L. (2014). Effect of fabric and weathering intensity on dynamic properties of residual and saprolitic soils via resonant column testing. *Geotechnical Testing Journal*, *37*(5). https://doi.org/10.1520/GTJ20120132

Pineda, J., Hoyos, L., & Colmenares, J. (2010). Stiffness Response of Residual and Saprolitic Soils Using Resonant Column and Bender Element Testing Techniques. *GeoFlorida 2010: Advances in Analysis, Modeling & Design, 41095*(July 2015), 783–792. https://doi.org/10.1061/41095(365)77

Pineda, J., & Pete, N. (2017). Effects on small-strain dynamic shear modulus from resonant column testing. In *2017 Congreso Internacional de Innovacion y Tendencias en Ingenieria (CONIITI)* (pp. 1–6). IEEE. https://doi.org/10.1109/CONIITI.2017.8273327

Pino, A. H. (2013). *Effect of Suction on Dynamic Properties of Unsaturated Soils At Small To Mid Shear Strain Amplitudes*. https://doi.org/10.1017/CBO9781107415324.004

Travasarou, T., Bray, J. D., & Abrahamson, N. A. (2003). Empirical attenuation relationship for Arias Intensity, *1155*(March 2002), 1133–1155. https://doi.org/10.1002/eqe.270